Histol Histopathol (2024) 39: 509-521

Histology and Histopathology
From Cell Biology to Tissue Engineering

ORIGINAL ARTICLE Open Access

ACAT2 negatively modulated by FOXA2 suppresses ferroptosis to expedite the aggressive phenotypes of endometrial cancer cells

Xin Xiao[1], Tingyun Huang[1], Bin Chen[2], Jinshu Zhu[3], Qingbang Xiao[4] and Yuxin Bao[1]

[1]Institute of Life Sciences, Zunyi Medical University, [2]Key Laboratory of Oral Disease of Higher Schools in Guizhou Province, Zunyi, [3]Department of Cerebral Surgery, Qiannan Prefecture Hospital of Traditional Chinese Medicine, Duyun and [4]Department of Pathology, Affiliated Hospital of Zunyi Medical University, Zunyi, Guizhou, China

Summary. Endometrial cancer (EC) remains a prevalent gynecological disease with a continuously rising incidence and fatality rate. Acyl coenzyme A: cholesterol acyltransferase 2 (ACAT2) has been commonly perceived as a tumor promoter in multiple human malignancies. This study was conducted to specify the role and mechanism of ACAT2 in EC, which has not been covered. The expression and prognostic significance of ACAT2 in EC samples were respectively analyzed by the ENCORI and Kaplan-Meier plotter databases. RT-qPCR and western blot examined ACAT2 and forkhead box protein A2 (FOXA2) expression in EC cells. The CCK-8 method, colony formation, and EdU staining assays detected cell proliferation. The cell cycle was detected by flow cytometry analysis. Wound healing and Transwell assays, respectively, estimated cell migration and invasion. The thiobarbituric acid reactive species (TBARS) method and BODIPY 581/591 C11 probe detected lipid peroxidation levels. FerroOrange staining estimated intracellular iron level. Western blot examined the expression of epithelial-mesenchymal transition (EMT) and ferroptosis-associated proteins. The human TFDB database predicted the binding of FOXA2 with the ACAT2 promoter, which was substantiated by ChIP and luciferase reporter assays. As a result, ACAT2 expression was increased in EC tissues and cells and associated with poor survival outcomes in EC patients. ACAT2 deletion might hinder EC cell proliferation, migration, invasion, and EMT while stimulating cell cycle arrest. Moreover, ACAT2 silencing promoted the ferroptosis of EC cells. Also, FOXA2 inactivated the transcription of ACAT2 through binding with the ACAT2 promoter. FOXA2 interference could promote the proliferation, migration, invasion, EMT, cell cycle, and inhibit the ferroptosis of ACAT2-silenced EC cells, which was partially reversed by the ferroptosis activator erastin. Conclusively, ACAT2 transcriptionally inactivated by FOXA2 might contribute to the malignant progression of EC via the inhibition of ferroptosis.

Key words: ACAT2, Endometrial cancer, Ferroptosis, FOXA2, Migration, Invasion

Corresponding Author: Yuxin Bao, Institute of Life Sciences, Zunyi Medical University, 6 Xuefu West Road, Xinpu New District, Zunyi, Guizhou 563000, China. e-mail: BaoxinyuDoc@163.com
www.hh.um.es. DOI: 10.14670/HH-18-793

Introduction

Endometrial cancer (EC) comprises a group of malignant epithelial tumors that arise from the female genital tract, especially in perimenopausal and postmenopausal women (Van Nyen et al., 2018). Accumulative risk factors, including prolonged unopposed estrogen exposure, obesity, and age, are recognized as responsible for the initiation of EC (Ali, 2013). As released by the International Agency for Research on Cancer (IARC) of the World Health Organization, the global cancer burden data supports that EC ranks 6th of all cancers in terms of morbidity, with approximately 417,000 new cases and 97,000 deaths in 2020 (Sung et al., 2021). In 2015, there were 63,400 newly emerged cases and 21,800 deaths of EC in China (Chen et al., 2016). Surgery, adjuvant chemotherapy and radiotherapy are recommended as standard therapies for EC, depending on tumor grade and stage (Colombo et al., 2013). As a consequence, the prognosis for patients with relapsed or advanced EC remains dismal based on clinical epidemiological data (Connor and Rose, 2018). In view of this, alternative treatment regimens for EC demand to be developed.

Acyl-coenzyme A (CoA): cholesterol acyltransferase (ACAT) is a resident endoplasmic reticulum enzyme that

produces cholesteryl ester by converting cholesterol and long-chain fatty acyl-CoA (Buhman et al., 2000). Acyl coenzyme A: cholesterol acyltransferase 2 (ACAT2), an isoform of the ACAT family primarily expressed in intestinal epithelial cells and liver cells, is associated with lipoprotein assembly and secretion (Joyce et al., 1999). Recent literature has increasingly uncovered the crucial role of ACAT2 in other human malignancies, including colorectal cancer (Weng et al., 2020), bladder cancer (Cheng et al., 2023), and esophageal squamous cell carcinoma (Heng et al., 2023). Nevertheless, whether ACAT2 is involved in EC is still unclear.

Forkhead box (FOX) proteins are a family of transcription factors involved in the regulation of diverse cellular processes in varying manners (Bach et al., 2018). As a member of the FOX family, forkhead box protein A2 (FOXA2) is aberrantly expressed in multiple adult tissues, exerting multifaceted functions in the pathogenesis and occurrence of various cancers (Myatt and Lam, 2007). In particular, FOXA2 has been proposed as a tumor suppressor in EC (Smith et al., 2016; Shi et al., 2017; Sahoo et al., 2022).

This paper aims to specify the role of ACAT2 associated with FOXA2 in the progression of EC.

Materials and methods

Bioinformatics tools

The ENCORI database (https://rnasysu.com/encori/) detected ACAT2 expression in EC tissues. The Kaplan-Meier plotter database (http://kmplot.com/analysis/index.php?p=background) conducted the survival analysis of ACAT2 in EC. The human TFDB database (http://bioinfo.life.hust.edu.cn/HumanTFDB/) predicted the binding of FOXA2 with the ACAT2 promoter.

Cell culture and treatment

Human normal endometrial stromal cells (ESC) and human EC cells, including HEC-1A, HEC-50, and Ishikawa (Bluefbio, Shanghai, Chin), were all cultivated in Dulbecco's modified Eagle's medium (DMEM; SUNNCELL, Wuhan, China) comprising 10% fetal bovine serum (FBS; SUNNCELL, Wuhan, China) in a 5% CO_2-enriched humidified atmosphere at 37°C. The ferroptosis activator erastin (5 μg/mL; Adooq Biosciences, USA) was utilized to treat HEC-50 cells for 24h (Zheng et al., 2023).

Transfection protocol

After the specific shRNA sequences for ACAT2 or FOXA2 (Sbo-Bio, Shanghai, China) were cloned into the pLKO.1 lentiviral vector (Addgene) and the amplified FOXA2 cDNA fragments were inserted into the pcDNA3.1 vector (Addgene), HEC-50 cells were transfected with the acquired sh-ACAT2#1/2, sh-FOXA2#1/2, or Ov-FOXA2 as well as the corresponding non-targeting negative control (sh-NC) and empty vector (Ov-NC) with the application of Lipofectamine 3000 (Life Technologies, Carlsbad, CA, USA) in line with the supplier's recommendations.

Cell counting kit-8 (CCK-8)

The transfected HEC-50 cells (5×10^3 cells/well) with or without treatment with erastin were inoculated into the 96-well plates. Then, each well was treated with 10 μl CCK-8 solution (Signalway Antibody LLC, College Park, MD, USA) at 37°C for an additional 2h, strictly based on the manual provided by the manufacturer. The absorbance at 450 nm was detected under a microplate reader (Wuxi Hiwell Diatek Instruments Co., Ltd., Jiangsu, China).

Colony formation assay

Transfected HEC-50 cells inoculated in 6-well plates (400 cells/well) were cultured at 37°C in the absence or presence of erastin. After 14 days, the colonies formed were fixed in 4% paraformaldehyde, dyed with 0.5% crystal violet, and then counted under a light microscope (KEYENCE, Osaka, Japan).

5-Ethynyl-2'-deoxyuridine (EdU) staining

Cell proliferation was measured via the employment of the BeyoClick EdU-555 kit (Beyotime, China). In brief, the transfected HEC-50 cells (5×10^4 cells/well) were inoculated into 96-well plates in the absence or presence of erastin and incubated with 20 μM EDU for 2h, in accordance with the operating manual. Afterward, cells were fixed in 4% paraformaldehyde and permeabilized with 0.5% Triton X-100, then cultivated with Click reaction buffer and stained with Hoechst 33342. Under a fluorescence microscope (KEYENCE, Osaka, Japan), the EdU-positive cells were imaged.

Flow cytometry analysis

After being trypsinized, the transfected HEC-50 cells with or without erastin treatment were fixed with 70% cold ethanol at 4°C and stained with propidium iodide (PI) containing RNase A for 30 min at 37°C protected from light at room temperature. Cell cycle distribution was analyzed by a flow cytometer (ACEA Biosciences, Inc.) with Software NovoExpress 1.4.0 (ACEA Biosciences, Inc.).

Wound healing assay

The transfected HEC-50 cells were inoculated into 6-well plates ($7x10^5$ cells/well) in the absence or presence of erastin. A wound was introduced into the middle of the well with a 200 μL micropipette tip when

cell confluency reached 70-80%. The spread of wound closure at 0h and 24h was documented under a light microscope.

Transwell assay

The suspension of the transfected HEC-50 cells (200 µl) in the absence or presence of erastin was added to the upper Transwell chambers paved with Matrigel (BD Biosciences, MA, USA). The undersides were filled with 500 µL medium with 10% FBS. After 24h, the remaining cells in the upper chamber were cleared by gentle scrubbing with a cotton swab while the cells that traveled to the bottom of the membrane were immobilized by methanol and stained with 0.1% crystal violet. The stained cells were counted under a light microscope.

Thiobarbituric acid-reactive substances (TBARS) assay

With the application of the TBARS Assay Kit (Shanghai Westang Biotech Co., Ltd., Shanghai, China), lipid peroxidation was estimated. After centrifugation at 1600×g for 10 min, the cell supernatants were mixed with 0.1% thiobarbituric acid and rotated for 10 min at 95°C. The absorbance at 450 nm was detected under a microplate reader.

C11 BODIPY 581/591 assay

Transfected HEC-50 cells with or without erastin treatment were labeled by 5 µM C11 BODIPY 581/591 probe (BIOFOUNT, Beijing, China) at 37°C protected from light for 1h. Following PBS washing, the lipid peroxidation was analyzed by a flow cytometer and was quantified by the ratio of emission at 510 nm vs. 590 nm.

Estimation of Fe^{2+} content

Transfected HEC-50 cells grown in conditioned medium in 24-well plates in the absence or presence of erastin were labeled with 1 µmol/l FerroOrange (BIOFOUNT, Beijing, China) for 30 min. The fluorescence was visualized under a fluorescent microscope.

Reverse transcription-quantitative PCR (RT-qPCR)

The total RNA isolated from cells by the Isogen reagent (Nippongene, Tokyo, Japan) was converted to cDNA with the aid of the First Strand cDNA Synthesis Kit (EnzyValley, Guangzhou, China). cDNA was then amplified by PCR employing the PreScript One-Step RT-Qpcr SYBR Green Kit (EnzyValley, Guangzhou, China), referring to cDNA as a template. Relative ACAT2 and FOXA2 expressions were calibrated in terms of the $2^{-\Delta\Delta Cq}$ approach. GAPDH functioned as a normalization gene.

Western blot

After cells were lysed in RIPA buffer (Biorigin, Beijing, China), the BCA method (Biorigin, Beijing, China) was adopted to estimate protein content. Subsequently, the proteins fractionated on 12% SDS-PAGE were transferred to PVDF membranes. The membranes were then sealed with 5% BSA and immunoblotted with primary antibodies (Abcam) prior to the addition of HRP-conjugated secondary antibody (ab6721; 1/2000; Abcam). The signals of the blots were developed by Super ECL Plus (Biorigin, Beijing, China), and the intensity was analyzed with ImageJ software (ImageJ 1.4, NIH, USA).

Chromatin immunoprecipitation (ChIP)

The ChIP assay was executed employing the EpiQuik Chromatin Immunoprecipitation Assay Kit (EpiGentek), following the standard protocol. Firstly, HEC-50 cells were treated with 1% formaldehyde. The acquired chromatin fragments by sonication were incubated with FOXA2 antibody (cat. no. ab256493; Abcam) or IgG antibody (cat. no. ab205718; Abcam) overnight. The abundance of ACAT2 promoter was analyzed by PCR.

Luciferase reporter assay

Via Lipofectamine 3000, HEC-50 cells were co-transfected with the wild-type (WT) or mutant-type binding sequences of the ACAT2 promoter cloned into pGL3 vectors (Addgene) and Ov-NC, Ov-FOXA2. After 48h, the luciferase activity was determined with the aid of the Dual Luciferase Reporter Assay Kit (Promega Corporation, Madison, WI, USA).

Statistical analyses

The values were reported as mean ± standard deviation (SD) from three independent experiments adopting GraphPad Prism 8 software (GraphPad Software, Inc.). Observed differences were viewed as statistically significant at $p<0.05$ with the employment of one-way ANOVA followed by Tukey's test.

Results

ACAT2 is overexpressed in EC and has a negative prognostic significance

As depicted by the ENCORI database in Figure 1A, ACAT2 presented significantly increased expression in EC tissues compared with normal tissues. The longer overall survival time was also observed in EC patients with lower ACAT2 expression, demonstrating the negative correlation between ACAT2 expression and disease outcome (Fig. 1B). In addition, RT-qPCR and

western blot examined ACAT2 expression in EC cells and the results implied that, in contrast with the ESC cell line, ACAT2 expression was elevated in HEC-1A, HEC-50, and Ishikawa cells, especially in HEC-50 cells (Fig. 1C). Accordingly, HEC-50 cells were used in the subsequent experiments.

ACAT2 deletion obstructs EC cell proliferation and stimulates cell cycle arrest

To evaluate the role of ACAT2 in EC cells, ACAT2 interference plasmids were transfected into HEC-50 cells to knock down ACAT2 prior to loss-of-function experiments. Predictably, ACAT2 expression exhibited a notable downward trend after transfection of sh-ACAT2#1/2 (Fig. 2A). In particular, sh-ACAT2#2 was selected for follow-up assays for its prominent interference efficacy. As illustrated in Figure 2B, the data from the CCK-8 assay expounded that the viability of HEC-50 cells declined markedly after ACAT2 was depleted. Also, it was noticed that the number of colonies was remarkably decreased when ACAT2 was downregulated (Fig. 2C). Furthermore, EdU staining revealed that the silencing of ACAT2 resulted in a prominent decline in EdU-positive cells (Fig. 2D). In addition, the results of flow cytometry analysis uncovered that after ACAT2 was knocked down, the proportion of cells in the G0/G1 phase was enhanced, while the proportion of cells in the S phase was reduced (Fig. 2E).

ACAT2 deletion hinders the migration, invasion, and EMT of EC cells

Moreover, through wound healing and Transwell assays, it turned out that the migratory and invasive abilities of HEC-50 cells were both greatly attenuated by the deficiency of ACAT2 (Fig. 3A,B). Additionally, the expression of EMT-associated proteins was analyzed by western blot, finding that E-cadherin protein expression was upregulated whilst N-cadherin and Snail protein expression were downregulated by interference with ACAT2 (Fig. 3C).

ACAT2 deletion accelerates the ferroptosis of EC cells

Simultaneously, it was noticed that after ACAT2 was silenced, TBARS production was significantly facilitated (Fig. 4A). Also, the lipid ROS and Fe2+ contents were both elevated by the absence of ACAT2 (Fig. 4B,C). Western blot analysis also indicated that SLC7A11 and GPX4 expression declined and ACSL4 and TFR1 expression were elevated by downregulation of ACAT2

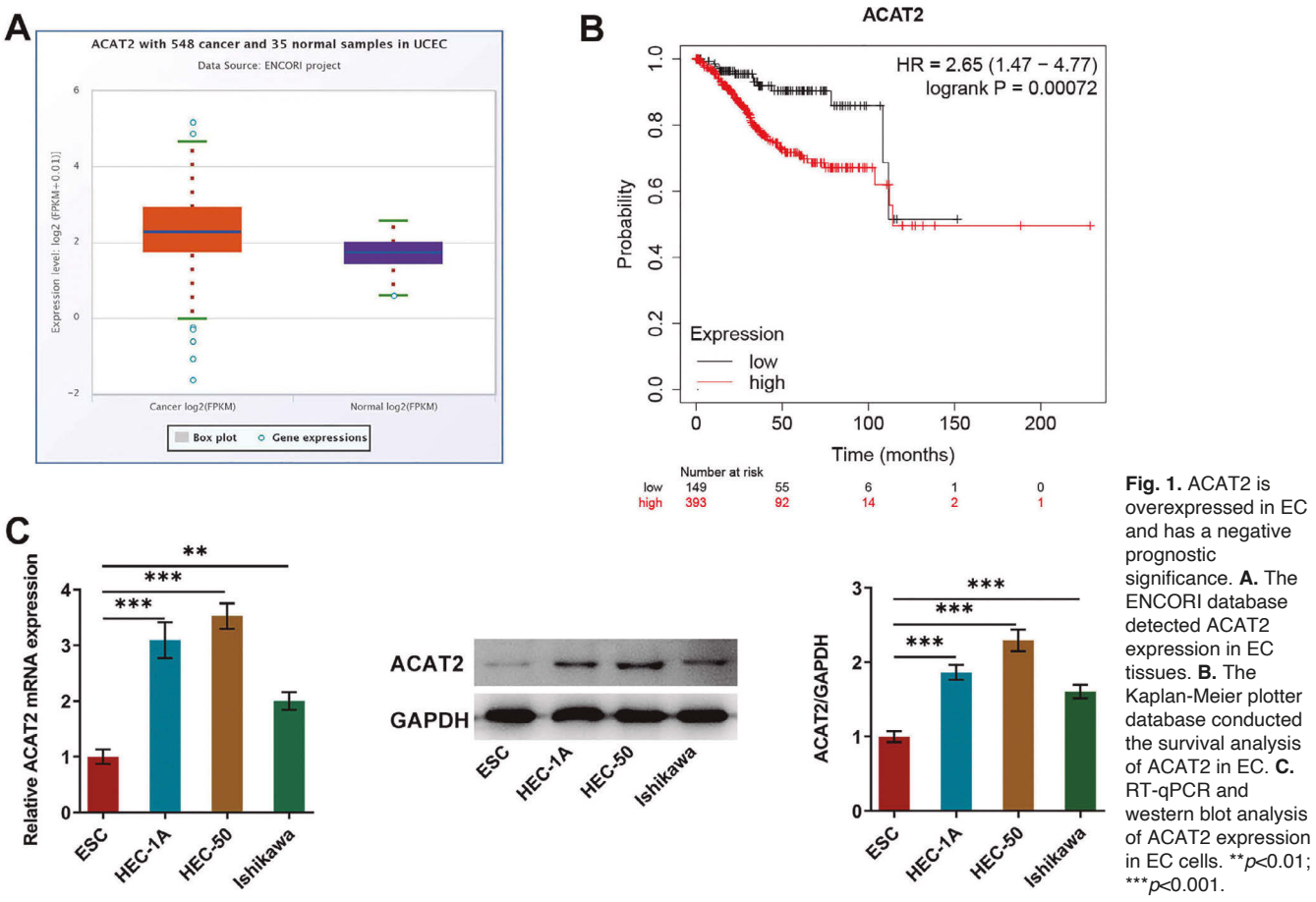

Fig. 1. ACAT2 is overexpressed in EC and has a negative prognostic significance. **A.** The ENCORI database detected ACAT2 expression in EC tissues. **B.** The Kaplan-Meier plotter database conducted the survival analysis of ACAT2 in EC. **C.** RT-qPCR and western blot analysis of ACAT2 expression in EC cells. **p<0.01; ***p<0.001.

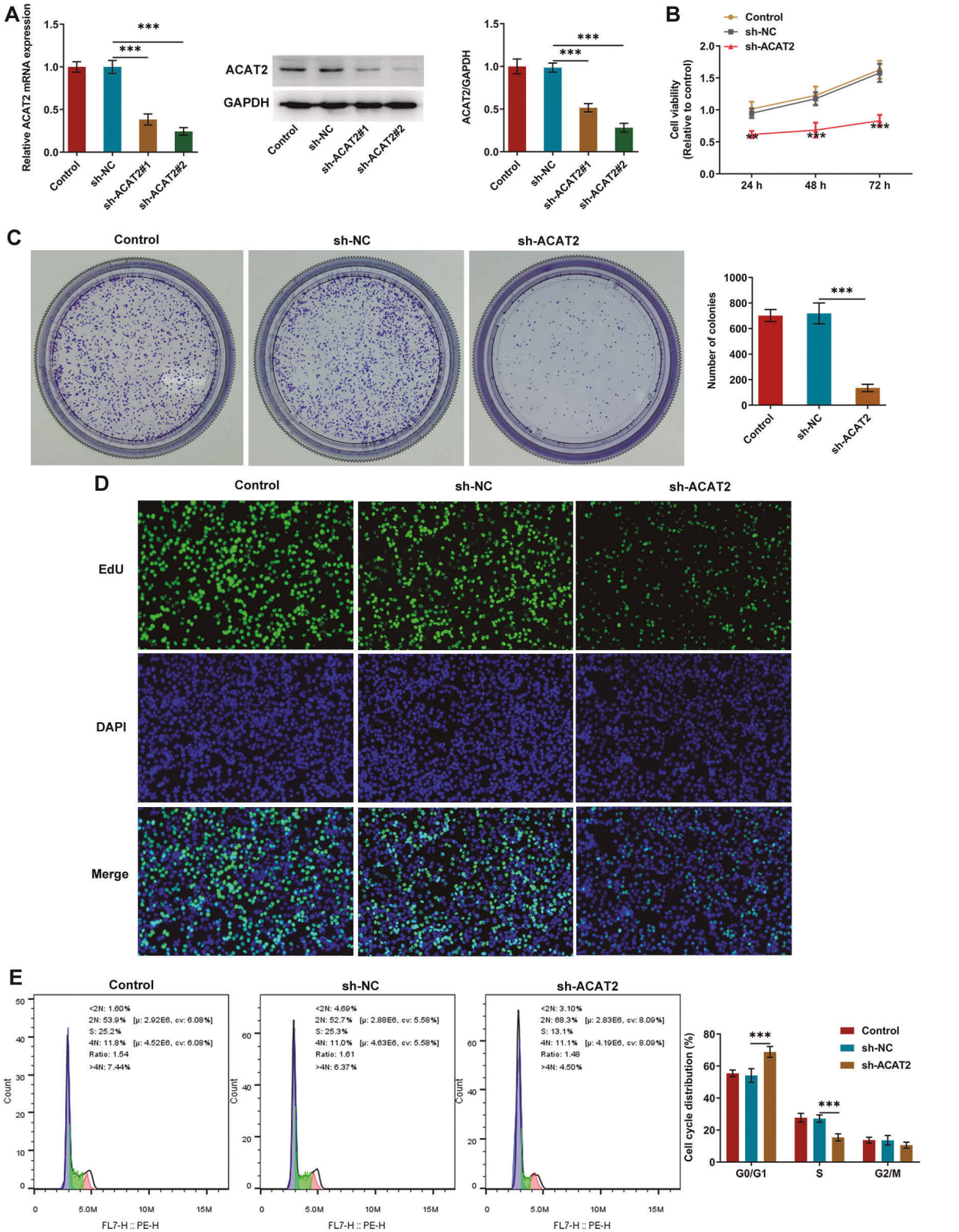

Fig. 2. ACAT2 deletion obstructs EC cell proliferation and stimulates cell cycle arrest. **A.** RT-qPCR and western blot analysis of ACAT2 expression after transfection of ACAT2 interference plasmids. **B.** Cell viability was detected via the CCK-8 method. **C.** Colony formation and **(D)** EdU staining assays were used to detect cell proliferation **(D)**. **E.** A Flow cytometry assay was used to detect the cell cycle. ***p<0.001.

(Fig. 4D).

FOXA2 binds with the ACAT2 promoter and inhibits the transcription of ACAT2

Based on the Human TFDB database, the possible binding sequences of FOXA2 with the ACAT2 promoter were predicted (Fig. 5A). Intriguingly, FOXA2 expression was discovered to be depleted in HEC-50 cells relative to ESC cells (Fig. 5B). After transfection of Ov-FOXA2 and sh-FOXA2#1/2 plasmids, FOXA2 expression was respectively improved and inhibited in HEC-50 cells (Fig. 5C). Notably, sh-FOXA2#2 was chosen for the ensuing experiments due to its significant interference efficacy. Meanwhile, the luciferase reporter assay confirmed that the upregulation of FOXA2 greatly reduced the luciferase activity of the ACAT2 promoter (Fig. 5D). The ChIP assay also revealed that the ACAT2 promoter was enriched in FOXA2 antibody. Further, RT-qPCR and western blot analysis underlined that ACAT2 expression was decreased by the elevation of FOXA2 and increased by FOXA2 insufficiency (Fig. 5E), suggesting the negative transcriptional regulation of ACAT2 by FOXA2.

Disturbance of FOXA2 reverses the impact of ACAT2 reduction on the ferroptosis of EC cells

As expected, the promoted TBARS production caused by ACAT2 knockdown in HEC-50 cells was noticeably suppressed by interference with FOXA2 (Fig.

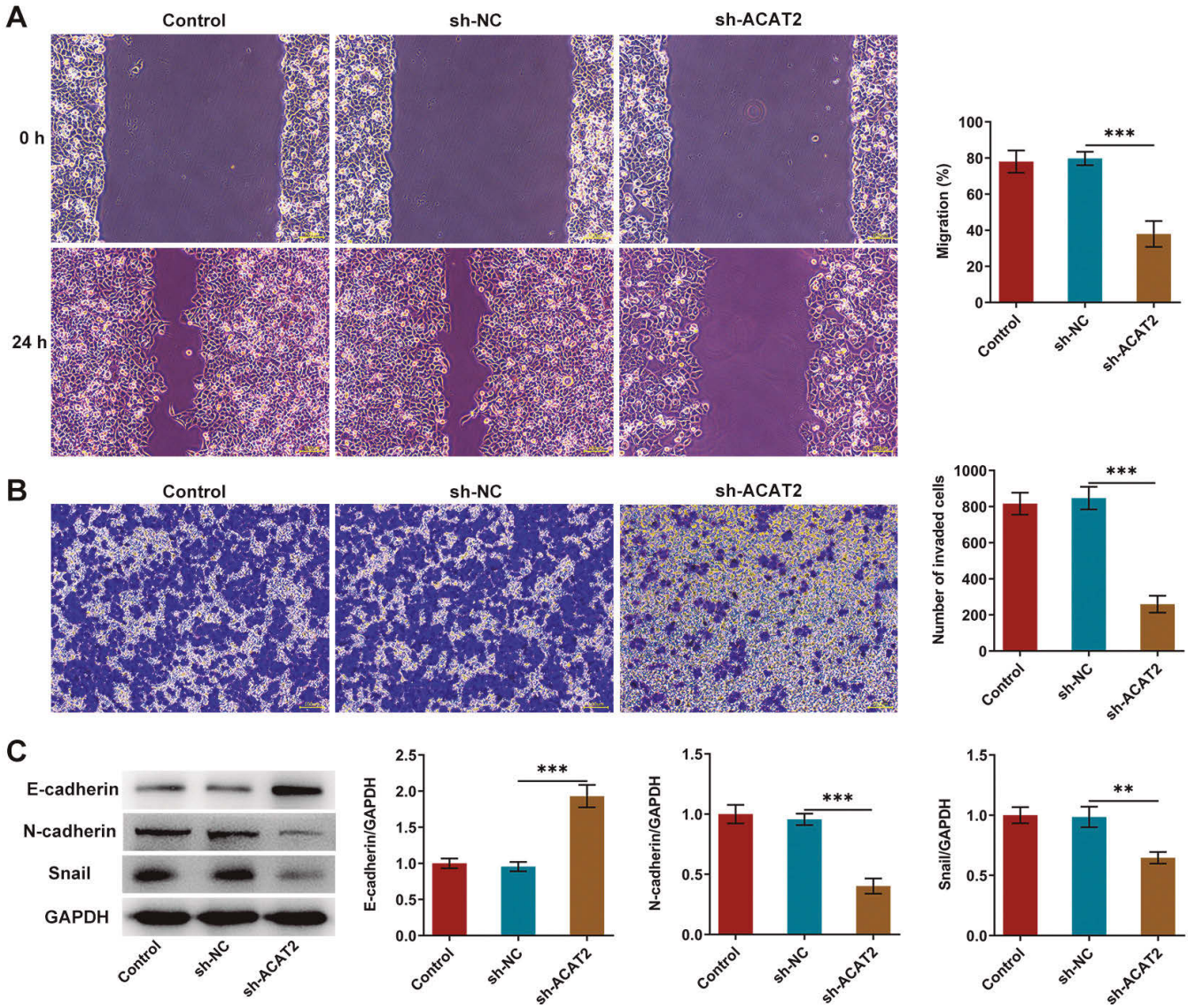

Fig. 3. ACAT2 deletion hinders the migration, invasion, and EMT of EC cells. **A.** A wound healing assay was used to detect cell migration. **B.** The Transwell assay was used to detect cell invasion. **C.** Western blot examined the expression of EMT-associated proteins. **p<0.01; ***p<0.001.

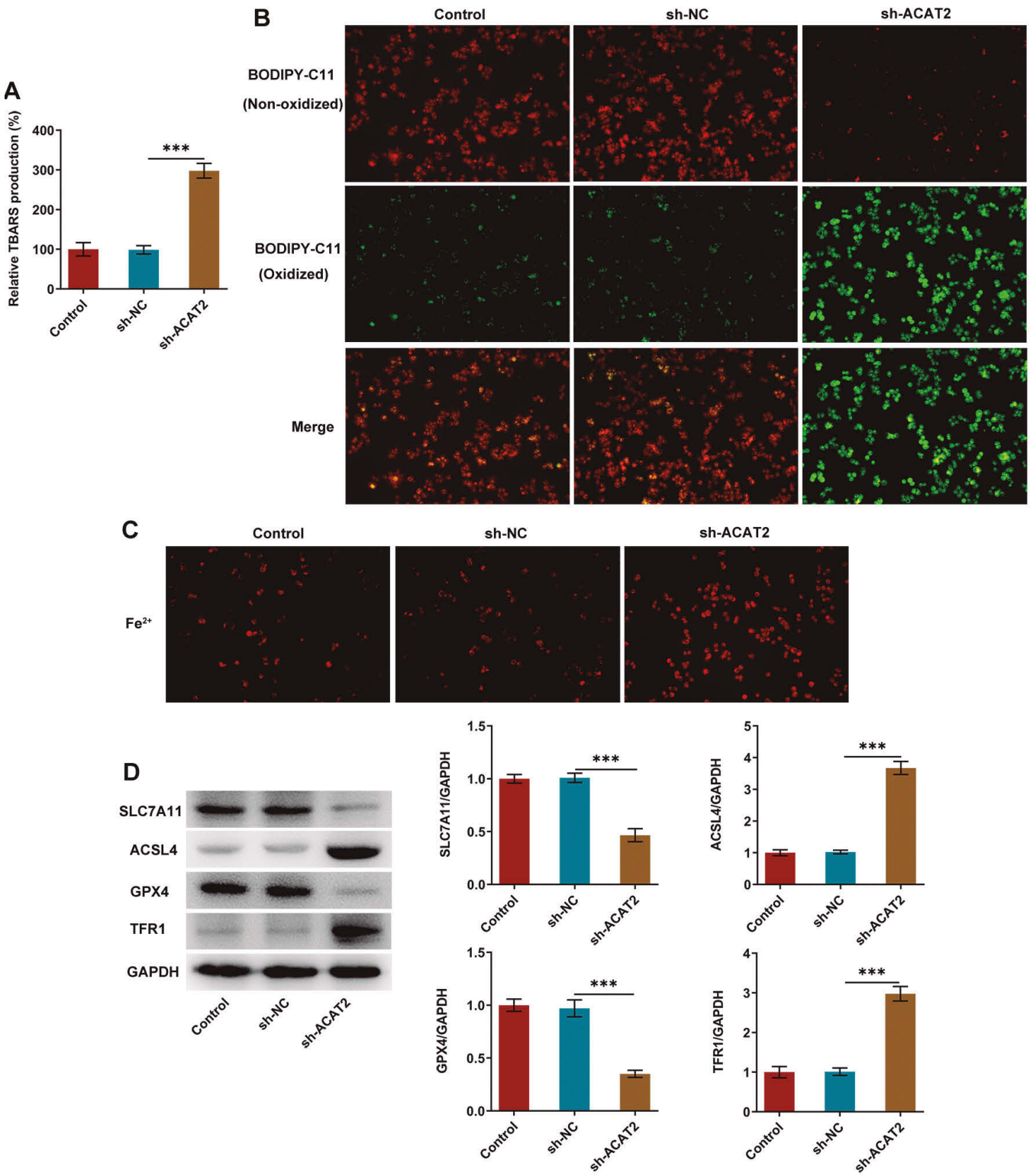

Fig. 4. ACAT2 deletion accelerates the ferroptosis of EC cells. **A.** The TBARS method estimated the TBARS production. **B.** The BODIPY 581/591 C11 probe estimated lipid ROS levels. **C.** FerroOrange staining estimated intracellular iron levels. **D.** Western blot examined the expression of ferroptosis-associated proteins. ***$p<0.001$.

6A). Also, downregulation of FOXA2 decreased the lipid ROS and Fe^{2+} contents, which were both enhanced in ACAT2-silencing HEC-50 cells (Fig. 6B,C). Deficiency of ACAT2 downregulated SLC7A11 and GPX4 expression and upregulated ACSL4 and TFR1 expression in HEC-50 cells, which were all reversed after FOXA2 was silenced (Fig. 6D).

Disturbance of FOXA2 reverses the impact of ACAT2 reduction on cell proliferation and cell cycle in EC through mediating ferroptosis

At the same time, pretreatment with the ferroptosis activator erastin partially repressed the viability that was accelerated in FOXA2-silenced and ACAT2-silenced HEC-50 cells (Fig. 7A). Likewise, the number of colonies and EdU-positive cells in the sh-ACAT2 + sh-FOXA2 group was distinctly enhanced compared with the sh-ACAT2 + sh-NC group, which was then reduced by erastin (Fig. 7B,C). Also, FOXA2 deletion reduced the cells in the G0/G1 phase and arrested more cells in the S phase in HEC-50 cells transfected with sh-ACAT2. Relative to the sh-ACAT2 + sh-FOXA2 group, the progression of HEC-50 cells from the G0/G1 phase to the S phase was inhibited in the sh-ACAT2 + sh-FOXA2 + Erastin group (Fig. 7D).

Disturbance of FOXA2 reverses the impact of ACAT2 reduction on cell migration, invasion, and EMT in EC through mediating ferroptosis

Concurrently, after pretreatment with erastin, the

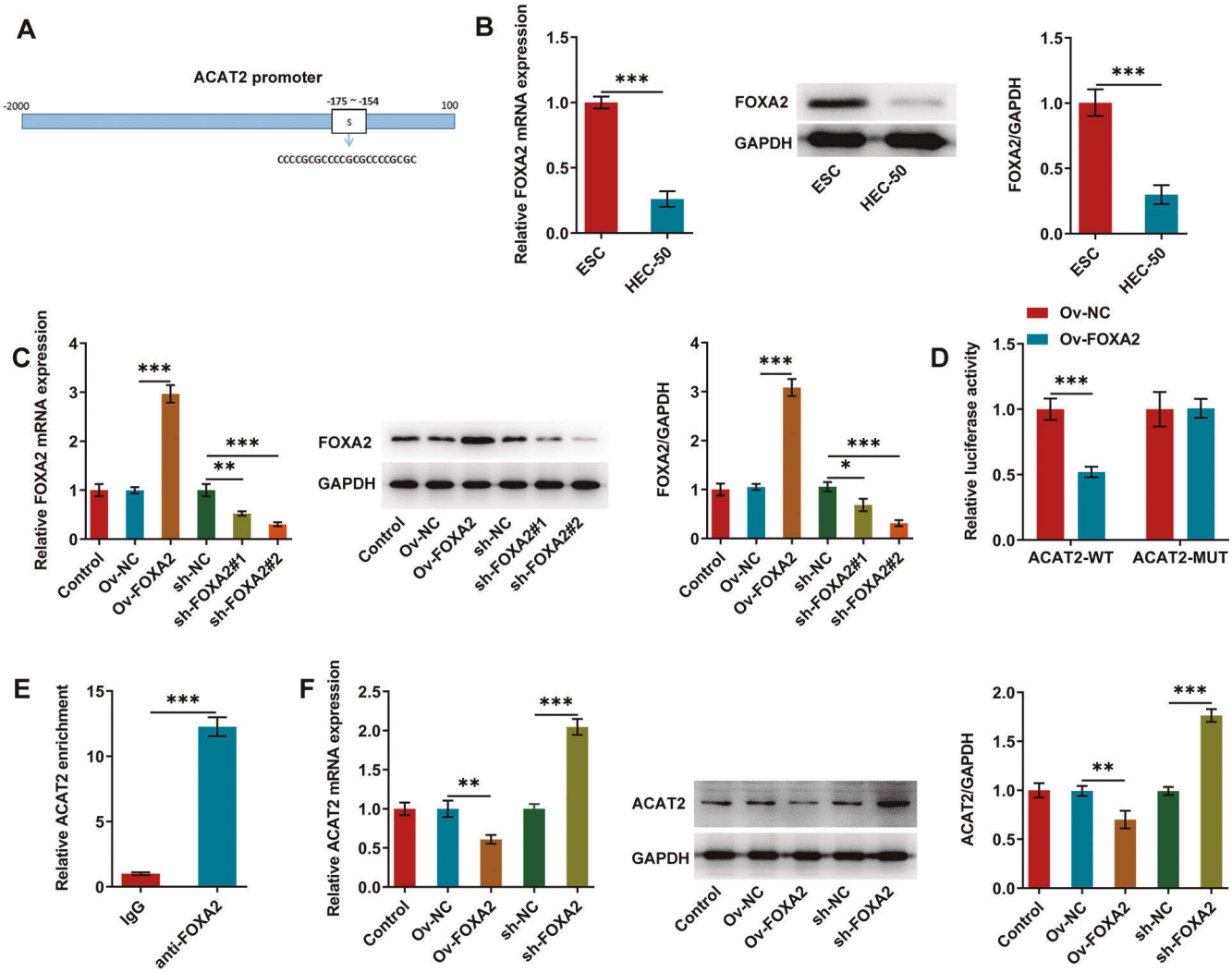

Fig. 5. FOXA2 binds with the ACAT2 promoter and inhibits the transcription of ACAT2. **A.** The predicted binding sites between FOXA2 and the ACAT2 promoter by the Human TFDB database. **B.** RT-qPCR and western blot analysis of FOXA2 expression in EC cells. **C.** RT-qPCR and western blot analysis of FOXA2 expression after transfection with FOXA2 overexpression interference plasmids. **D.** Luciferase reporter assay assessed the luciferase activity of the ACAT2 promoter. **E.** The ChIP assay assessed the abundance of ACAT2 promoter in the FOXA2 antibody. **F.** RT-qPCR and western blot analysis of ACAT2 expression after transfection with FOXA2 overexpression interference plasmids. $^{**}p<0.01$; $^{***}p<0.001$.

promoted migratory and invasive abilities in ACAT2-silenced HEC-50 cells due to the absence of FOXA2 were both reduced (Fig. 8A,B). Knockdown of FOXA2 reduced E-cadherin protein expression whereas increased N-cadherin and Snail protein expression in HEC-50 cells transfected with sh-ACAT2, which was then reverted by erastin (Fig. 8C).

Discussion

EC is commonly deemed to arise through progressive accumulation of multiple genetic abnormalities, which may activate oncogenes and inactivate tumor-suppressor genes (Yanokura et al., 2017). In addition to the important role of ACAT2 in intracellular cholesterol homeostasis (Long et al., 2021), ACAT2 expression is also frequently dysregulated in tumors. For instance, ACAT2 is highly expressed in colorectal cancer tissue and correlated with tumor size, lymph node metastasis, clinical stage, and poor overall survival rate of colorectal cancer patients (Weng et al., 2020). Conversely, Zhao et al. supported that ACAT2 is downregulated in clear cell renal cell carcinoma and is related to tumor stage, size, and cancer-specific survival (Zhao et al., 2016). In our study, ACAT2 was also noted to be overexpressed in EC tissues and cells and could be established as a negative prognostic biomarker of EC through bioinformatics tools. Considering the pro-tumor

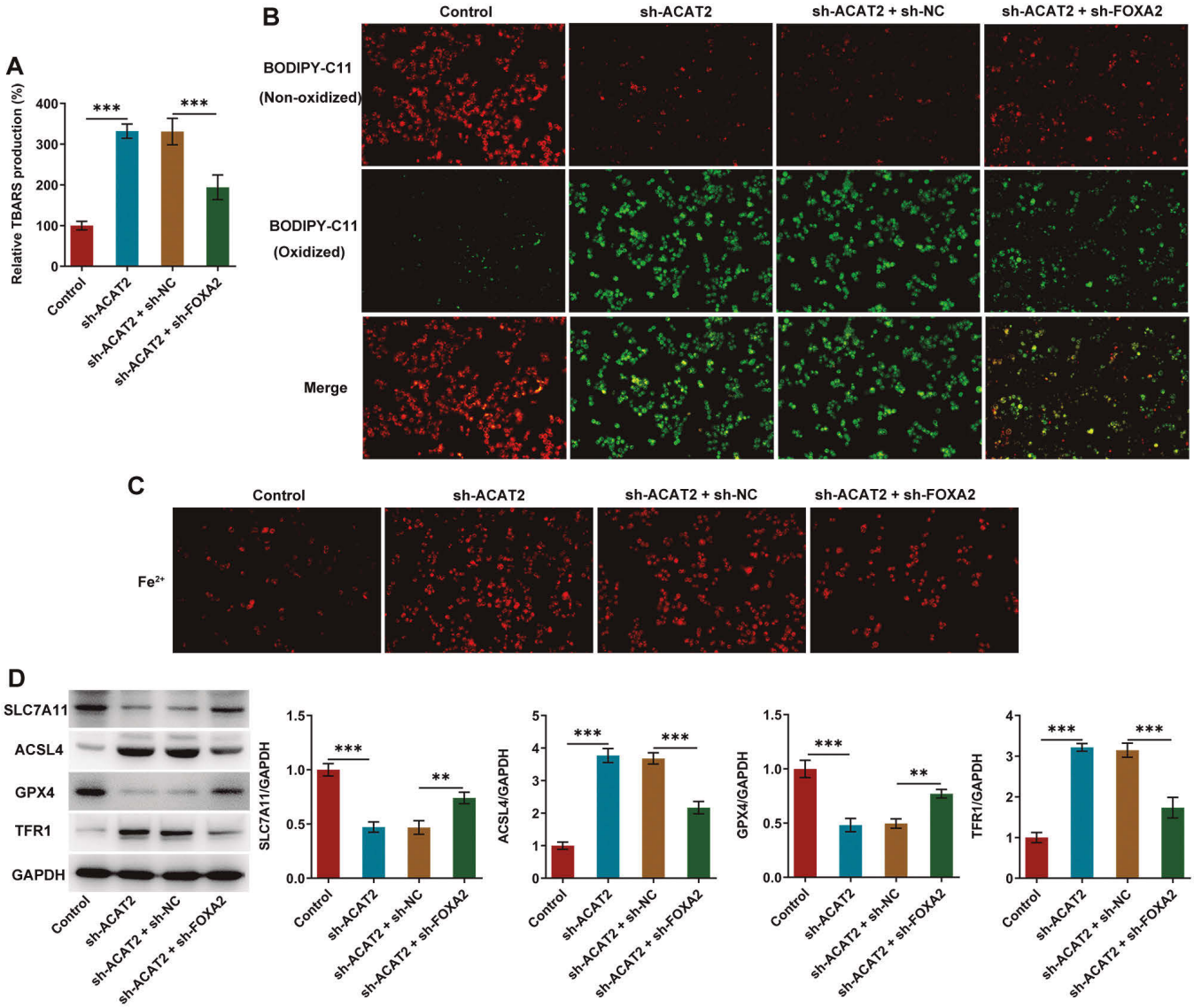

Fig. 6. Disturbance of FOXA2 reverses the impact of ACAT2 reduction on the ferroptosis of EC cells. **A.** The TBARS method estimated TBARS production. **B.** The BODIPY 581/591 C11 probe estimated lipid ROS levels. **C.** FerroOrange staining estimated intracellular iron levels. **D.** Western blot examined the expression of ferroptosis-associated proteins. **p<0.01; ***p<0.001.

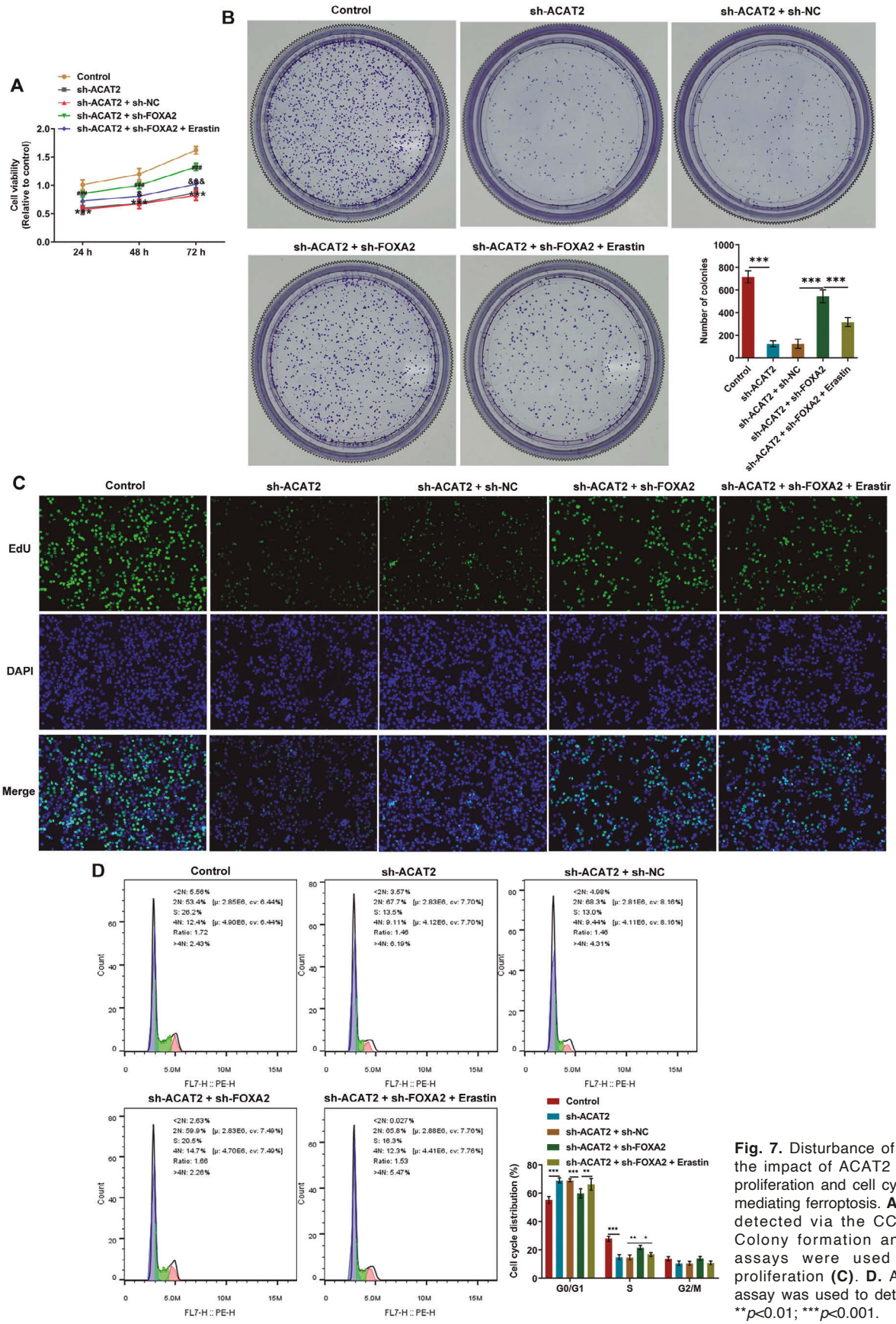

Fig. 7. Disturbance of FOXA2 reverses the impact of ACAT2 reduction on cell proliferation and cell cycle in EC through mediating ferroptosis. **A.** Cell viability was detected via the CCK-8 method. **B.** Colony formation and EdU staining assays were used to detect cell proliferation **(C)**. **D.** A Flow cytometry assay was used to detect the cell cycle. $^{**}p<0.01$; $^{***}p<0.001$.

or anti-tumor properties of ACAT2 by modulating the aggressive behaviors of colorectal, and bladder cancer cells, such as proliferation, apoptosis, cell cycle, migration, invasion, etc. (Weng et al., 2020; Cheng et al., 2023), we observed that knockdown of ACAT2 evidently suppressed cell proliferation, migration, and invasion, and induced cell cycle arrest in EC. A widely accepted notion is that EMT is a phenotypic plasticity process that confers migratory and invasive properties to epithelial cells during the pathogenesis of EC (Chiu et al., 2019). The loss of epithelial markers of tumor cells, such as E-cadherin, and the acquisition of mesenchymal markers, such as N-cadherin, are markers of EMT occurrence (Loh et al., 2019). Snail, an E-cadherin suppressor, functions primarily as an EMT inducer (Wang et al., 2013). As reported, ACAT2 knockdown partly restores the suppressive role of miR-1233 down-regulation in the EMT of clear cell renal cell carcinoma cells (Cheng et al., 2021). On the contrary, in the current paper, it turned out that ACAT2 might serve as a driver of EMT in EC, which was manifested by the upregulated E-cadherin expression and downregulated N-cadherin and Snail expression in HEC-50 cells when ACAT2 was depleted.

Ferroptosis is a non-apoptotic form of programmed cell death mode that occurs as a consequence of iron-dependent, intracellular ROS accumulation (Jiang et al., 2021). It is known that ferroptosis plays an essential role in the progression and drug resistance of aggressive tumor types, including EC, and ferroptosis induction is regarded as a promising anticancer strategy (Liang et al., 2019; Mou et al., 2019; Wu et al., 2022). The deposition of lipid peroxidation yielded by the excessive accumulation of iron in the cytoplasm is viewed as the landmark event of ferroptosis (Rochette et al., 2022). SLC7A11 mainly takes charge of the import of extracellular cystine into the cells, which is critical to the synthesis of glutathione (GSH). GPX4 can detoxify lipid peroxides to lipid alcohols, adopting GSH as a cofactor, thus being identified as a negative regulator of ferroptosis (Yang et al., 2014). ACSL4 is a member of the long-chain family of acyl-CoA synthetase proteins

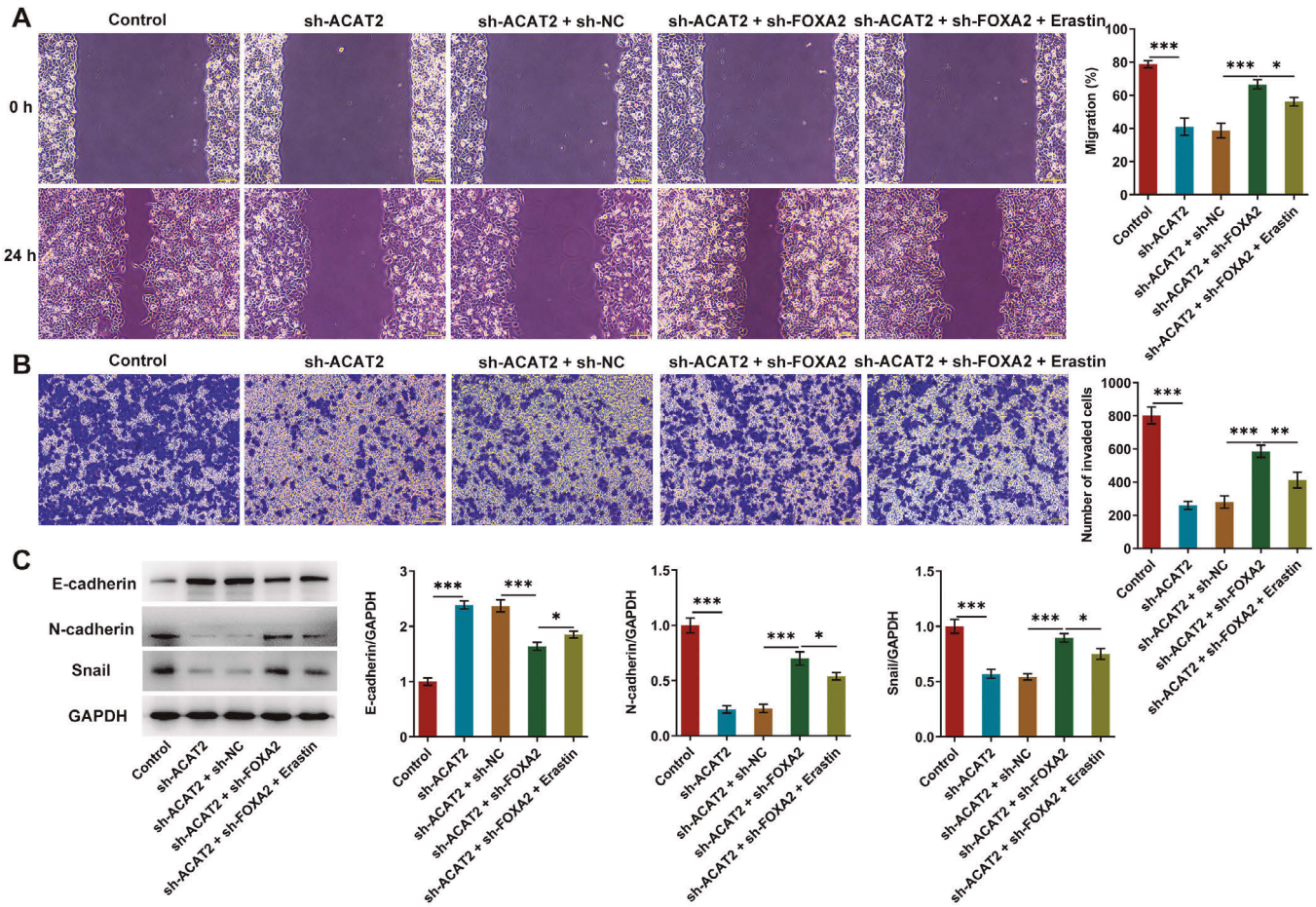

Fig. 8. Disturbance of FOXA2 reverses the impact of ACAT2 reduction on cell migration, invasion, and EMT in EC through mediating ferroptosis. **A.** A wound healing assay was used to detect cell migration. **B.** The Transwell assay was used to detect cell invasion. **C.** Western blot examined the expression of EMT-associated proteins. *p<0.05; **p<0.01; ***p<0.001.

that activate long-chain fatty acids for the synthesis of cellular lipids, and TFR1 charges cellular iron uptake (Yuan et al., 2016; Feng et al., 2020). Interestingly, Heng et al. have held the opinion that ACAT2 inactivates ferroptosis to confer the radioresistance of esophageal squamous cell carcinoma cells (Heng et al., 2023). Through investigation, the present study revealed that when ACAT2 was depleted, TBARS production, lipid ROS, and Fe^{2+} contents were all stimulated, accompanied by the reduced expression of ferroptosis suppressors SLC7A11 and GPX4 and the elevated expression of ferroptosis markers ACSL4, TFR1.

Through the Human TFDB database, it was predicted that FOXA2, a pioneer transcription factor, might be a transcriptional regulator of ACAT2, which was shown in the current work. Further experiments also uncovered that FOXA2 could bind to the ACAT2 promoter and negatively modulate ACAT2 expression in EC cells. Existing research has mentioned that FOXA2 is lowly expressed in EC cells and may serve as an endometrial tumor suppressor via inhibition of EMT (Shi et al., 2017; Sahoo et al., 2022). Further literature has highlighted that FOXA2 is implicated in the ferroptosis of colorectal cancer cells (Ma et al., 2023). The findings in the present work also disclosed the depleted FOXA2 expression in EC cells. When FOXA2 was downregulated, the promoted ferroptosis, cell cycle arrest, and inhibited proliferation, migration, invasion, as well as EMT of EC cells imposed by ACAT2 deletion were all partially reversed. Activation of ferroptosis might further abolish the impact of FOXA2 deficiency on the proliferation, cell cycle, migration, invasion, and EMT of ACAT2-silenced EC cells.

Collectively, ACAT2 reduction might retard the progression of EC via induction of ferroptosis, presenting that ACAT2 transcriptionally inhibited by FOXA2 might act as a promising therapeutic biomarker of EC and may be useful in the development of ferroptosis-based cancer therapy.

Funding. This work was funded by the Science and Technology Fund Project of Guizhou Provincial Health Commitee (gzwkj2024-275) and Guizou Province Science and Technology Program (Qianke Heji-ZK[2024] General 279).

References

Ali A.T. (2013). Risk factors for endometrial cancer. Ceska Gynekol. 78, 448-459.

Bach D.H., Long N.P., Luu T.T., Anh N.H., Kwon S.W. and Lee S.K. (2018). The dominant role of forkhead box proteins in cancer. Int. J. Mol. Sci. 19, 3279.

Buhman K.F., Accad M. and Farese R.V. (2000). Mammalian acyl-CoA:cholesterol acyltransferases. Biochim. Biophys. Acta 1529, 142-154.

Chen W., Zheng R., Baade P.D., Zhang S., Zeng H., Bray F., Jemal A., Yu X.Q. and He J. (2016). Cancer statistics in china, 2015. CA Cancer J. Clin. 66, 115-132.

Cheng L., Cao H., Xu J., Xu M., He W., Zhang W., Dong L. and Chen D. (2021). Circ_RPL23A acts as a miR-1233 sponge to suppress the progression of clear cell renal cell carcinoma by promoting ACAT2. J. Bioenerg. Biomembr. 53, 415-428.

Cheng Y., Yu H., Li K., Lv J., Zhuang J., Bai K., Wu Q., Yang X., Yang H. and Lu Q. (2023). Hsa_circ_0003098 promotes bladder cancer progression via miR-377-5p/ACAT2 axis. Genomics 115, 110692.

Chiu H.C., Li C.J., Yiang G.T., Tsai A.P. and Wu M.Y. (2019). Epithelial to mesenchymal transition and cell biology of molecular regulation in endometrial carcinogenesis. J. Clin. Med. 8, 439.

Colombo N., Preti E., Landoni F., Carinelli S., Colombo A., Marini C. and Sessa C. (2013). Endometrial cancer: ESMO clinical practice guidelines for diagnosis, treatment and follow-up. Ann. Oncol. 24 (Suppl. 6), vi33-38.

Connor E.V. and Rose P.G. (2018). Management strategies for recurrent endometrial cancer. Expert Rev. Anticancer Ther. 18, 873-885.

Feng H., Schorpp K., Jin J., Yozwiak C.E., Hoffstrom B.G., Decker A.M., Rajbhandari P., Stokes M.E., Bender H.G., Csuka J.M., Upadhyayula P.S., Canoll P., Uchida K., Soni R.K., Hadian K. and Stockwell B.R. (2020). Transferrin receptor is a specific ferroptosis marker. Cell Rep. 30, 3411-3423.e3417.

Heng J., Li Z., Liu L., Zheng Z., Zheng Y., Xu X., Liao L., Xu H., Huang H., Li E. and Xu L. (2023). Acetyl-coa acetyltransferase 2 confers radioresistance by inhibiting ferroptosis in esophageal squamous cell carcinoma. Int. J. Radiat. Oncol. Biol. Phys. 117, 966-978.

Jiang X., Stockwell B.R. and Conrad M. (2021). Ferroptosis: Mechanisms, biology and role in disease. Nat. Rev. Mol. Cell Biol. 22, 266-282.

Joyce C., Skinner K., Anderson R.A. and Rudel L.L. (1999). Acyl-coenzyme A:Cholesteryl acyltransferase 2. Curr. Opin. Lipidol. 10, 89-95.

Liang C., Zhang X., Yang M. and Dong X. (2019). Recent progress in ferroptosis inducers for cancer therapy. Adv. Mater. 31, e1904197.

Loh C.Y., Chai J.Y., Tang T.F., Wong W.F., Sethi G., Shanmugam M.K., Chong P.P. and Looi C.Y. (2019). The e-cadherin and n-cadherin switch in epithelial-to-mesenchymal transition: Signaling, therapeutic implications, and challenges. Cells 8, 1118.

Long T., Liu Y. and Li X. (2021). Molecular structures of human ACAT2 disclose mechanism for selective inhibition. Structure 29, 1410-1418.e1414.

Ma X., Xu M., Zhang X., Wang X., Su K., Xu Z., Wang X. and Yang Y. (2023). Gambogenic acid inhibits proliferation and ferroptosis by targeting the mir-1291/FOXA2 and AMPKα/SLC7A11/GPX4 axis in colorectal cancer. Cell Biol. Int. 47, 1813-1824.

Mou Y., Wang J., Wu J., He D., Zhang C., Duan C. and Li B. (2019). Ferroptosis, a new form of cell death: Opportunities and challenges in cancer. J. Hematol. Oncol. 12, 34.

Myatt S.S. and Lam E.W. (2007). The emerging roles of forkhead box (Fox) proteins in cancer. Nat. Rev. Cancer 7, 847-859.

Rochette L., Dogon G., Rigal E., Zeller M., Cottin Y. and Vergely C. (2022). Lipid peroxidation and iron metabolism: Two corner stones in the homeostasis control of ferroptosis. Int. J. Mol. Sci. 24, 449.

Sahoo S.S., Ramanand S.G., Gao Y., Abbas A., Kumar A., Cuevas I.C., Li H.D., Aguilar M., Xing C., Mani R.S. and Castrillon D.H. (2022). FOXA2 suppresses endometrial carcinogenesis and epithelial-mesenchymal transition by regulating enhancer activity. J. Clin. Invest. 132, e157574.

Shi W., Wang X., Ruan L., Fu J., Liu F. and Qu J. (2017). MiR-200a promotes epithelial-mesenchymal transition of endometrial cancer

cells by negatively regulating FOXA2 expression. Pharmazie 72, 694-699.

Smith B., Neff R., Cohn D.E., Backes F.J., Suarez A.A., Mutch D.G., Rush C.M., Walker C.J. and Goodfellow P.J. (2016). The mutational spectrum of FOXA2 in endometrioid endometrial cancer points to a tumor suppressor role. Gynecol. Oncol. 143, 398-405.

Sung H., Ferlay J., Siegel R.L., Laversanne M., Soerjomataram I., Jemal A. and Bray F. (2021). Global Cancer Statistics 2020: GLOBOCAN estimates of incidence and mortality worldwide for 36 cancers in 185 countries. CA Cancer J. Clin. 71, 209-249.

Van Nyen T., Moiola C.P., Colas E., Annibali D. and Amant F. (2018). Modeling endometrial cancer: Past, present, and future. Int. J. Mol. Sci. 19, 2348.

Wang Y., Shi J., Chai K., Ying X. and Zhou B.P. (2013). The role of snail in EMT and tumorigenesis. Curr. Cancer Drug Targets 13, 963-972.

Weng M., Zhang H., Hou W., Sun Z., Zhong J. and Miao C. (2020). ACAT2 promotes cell proliferation and associates with malignant progression in colorectal cancer. Onco Targets Ther. 13, 3477-3488.

Wu J., Zhang L., Wu S. and Liu Z. (2022). Ferroptosis: Opportunities and challenges in treating endometrial cancer. Front. Mol. Biosci. 9, 929832.

Yang W.S., SriRamaratnam R., Welsch M.E., Shimada K., Skouta R., Viswanathan V.S., Cheah J.H., Clemons P.A., Shamji A.F., Clish C.B., Brown L.M., Girotti A.W., Cornish V.W., Schreiber S.L. and Stockwell B.R. (2014). Regulation of ferroptotic cancer cell death by GPX4. Cell 156, 317-331.

Yanokura M., Banno K., Kobayashi Y., Nomura H., Hayashi S., Tominaga E. and Aoki D. (2017). Recent findings on epigenetic gene abnormalities involved in uterine cancer. Mol. Clin. Oncol. 7, 733-737.

Yuan H., Li X., Zhang X., Kang R. and Tang D. (2016). Identification of ACSL4 as a biomarker and contributor of ferroptosis. Biochem. Biophys. Res. Commun. 478, 1338-1343.

Zhao Z., Lu J., Han L., Wang X., Man Q. and Liu S. (2016). Prognostic significance of two lipid metabolism enzymes, HADHA and ACAT2, in clear cell renal cell carcinoma. Tumour Biol. 37, 8121-8130.

Zheng S., Mo J., Zhang J. and Chen Y. (2023). HIF-1α inhibits ferroptosis and promotes malignant progression in non-small cell lung cancer by activating the Hippo-YAP signalling pathway. Oncol. Lett. 25, 90.

Accepted July 11, 2024